On the use of marker data to determine the kinetics of the digestive behaviour of feeds

J. A. Belward[1]   J. S. Hanan[2]   B. A. Williams[3]
W. J. J. Gerrits[4]   M. J. Gidley[5]

(Received 14 November 2012; revised 3 October 2013)

Abstract

A model of the transport process that follows the progress of digesta successively through the small intestine of a monogastric is investigated. The process is multi-phase and multi-constituent, as described in detail by Bastianelli et al. [*J. Anim. Sci.*, 74:1873–1887, 1996]. The model describes the movement of marker substances that are used to obtain data on the interactions between the intestinal sections and digesta with differing levels of soluble fibre. A multi-stage process is modelled by a set of coupled first order linear differential equations. Solutions of steady and initial value problems provide information on the transfer rates of the processes. Properties of the solutions as functions of system parameters are examined.

Contents

1 Introduction

A model is constructed to investigate the mechanisms of digestion in mono-gastric animals. The aim is to simulate the transport of digesta successively through the stomach, small intestine and large intestine. Digesta is a mixture of a liquid and a viscoelastic solid which changes as it passes through the system. There are many reactions which occur within the digesta itself in relation to the surrounding intestinal tissue, and in relation to the materials absorbed from the digesta into the circulatory and lymphatic systems, and even feedback signals involving other organs [3, for further detail]. Recent experiments at the Gatton campus of The University of Queensland (UQ)

supplied data from 30 grower pigs fed five different experimental diets. Measurements were made of material and biochemical properties at multiple locations in the digestive systems. To obtain information on the progress of the digesta, inert marker compounds were included in the diets. The markers were either attached to inert dietary constituents, or remained in the liquid phase. We discuss how a linear model is used to determine the mass transfer rates in the small intestine from the progress of the markers. We introduce delays into the linear systems and investigate the analytic and numerical properties of these models. A similar system for particular rates without delays was described by Mazanov and Nolan [5], and Mazanov [6] conducted a general treatment of linear equations with delays. Changes in the time variable enable the delay terms to be eliminated and positive rates lead to a stable system. France et al. [4] examined analytical solutions of similar models. Work on the practical aspects of fitting the data will be reported elsewhere.

In Section 2 the model is described and some initial conclusions are drawn leading to the incorporation of delay elements. Further properties are investigated in Section 3 where dependence on the rate parameters and conservation of mass are addressed. The issue of mass distribution as a result of the delays is analysed and quantified in Section 4. Finally, in Section 5 consideration of the long term behaviour of the system leads to an important conclusion relating the steady state masses to the rate parameters.

2   The models

The digestive system is described as a four stage computational model with the stomach, two stages of the small intestine and the large intestine as separate entities, as discussed by Bastianelli et al. [2, p. 1874]. The purpose of the current investigation is to work towards developing similar models that capture the digestive processes in a way which matches the results of the UQ experiments. Such models have abstract structures and Renton et al. [1] used
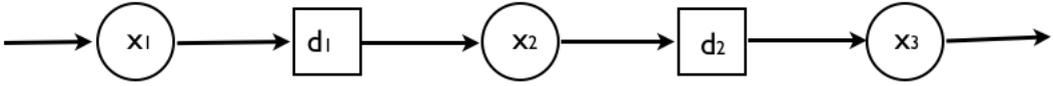
Figure 1:   A flow diagram of the model showing arcs, nodes (containing mass x_i) and delay elements (d_i).

such features for the functional-structural models of plants. These comprise nodes and arcs yielding time dependent differential equations which may be linear or nonlinear, depending on the interactions portrayed.

We aim to understand how the digesta moves through the small intestine. The data are measurements of the mass of four markers in six separate sections, or stages, the first and last being $1\,\mathrm{m}$ in length and the remainder roughly $3\,\mathrm{m}$. We model the behaviour of a typical marker and use this as a prototype for the marker which was fed to the animals over a period of three weeks, long enough to be regarded as having reached a steady state. The data on the remaining markers is then used to validate the model and provide further information.

Being inert, the multistage progress of the markers is depicted by a simple one dimensional scheme, as shown in Figure 1. This is an extract from the network of Bastianelli et al. [2] with delay elements inserted. The variable x_i denotes the marker mass present at the ith stage and its rate of change a_i is assumed proportional to the difference of the transport of mass in and mass out. All references to mass are to the mass of the marker whose function is to provide information on the movement of the digesta through the system. At the first stage the input of mass corresponds to the animal feeding. In Figure 1, boxes labelled with d_i represent a delay in the passage of mass from stage i to stage $i+1$. In the model, each equation is a statement of mass balance in terms of mass transfer. The results described here are generally independent of the number of stages, although the UQ experiment has six stages. Here we use as many as required to exemplify our results.

Using the marker data, our aim is to track the mass of digesta along the

entire small intestine. The retention time, (the duration of time for which mass is present in the stage in question) in each stage of the system (for each constituent) is important and we want to understand its relation to the mass transfer rates a_i. First order linear differential equations are given by Bastienelli et al. [2] for movement of the constituents through the system. With an arbitrary number of stages n the governing equations for $x_i(t)$, $i = 1, 2, \ldots, n$, are

$$\frac{dx_1}{dt} = f - a_1 x_1 \,, \tag{1}$$

$$\frac{dx_2}{dt} = a_1 x_1(t - d_1) - a_2 x_2 \,, \tag{2}$$

$$\frac{dx_i}{dt} = a_{i-1} x_{i-1}(t - d_{i-1}) - a_i x_i \,, \tag{3}$$

$$\frac{dx_n}{dt} = a_{n-1} x_{n-1}(t - d_{n-1}) - a_n x_n \,. \tag{4}$$

With initial values and delays d_i set to zero, for a four stage system we obtain the solutions portrayed in Figure 2. We get an idea of the retention time by setting a threshold that corresponds to the smallest mass experimentalists can measure and thereby estimate the width of the plots in Figure 2 (which are, theoretically, unbounded). We address this issue later; however, it is enough to state here that a working hypothesis is that we can use the reciprocals of the retention times to approximate the rates. This model is useful but not accurate as the whole system starts up immediately. A simple remedy to deal with this issue is to introduce delays between successive nodes and consider the amount moving past a point rather than in the nodes. Figure 1 is a schematic portrayal of this model and the relevant equations are (1)–(4) with nonzero d_i. The delays can be specified at particular times or evaluated as the system is integrated. Since the right hand sides of equations (1)–(4) are mass transfer rates we activate stage $i + 1$ according to the mass x_i present at the ith node.
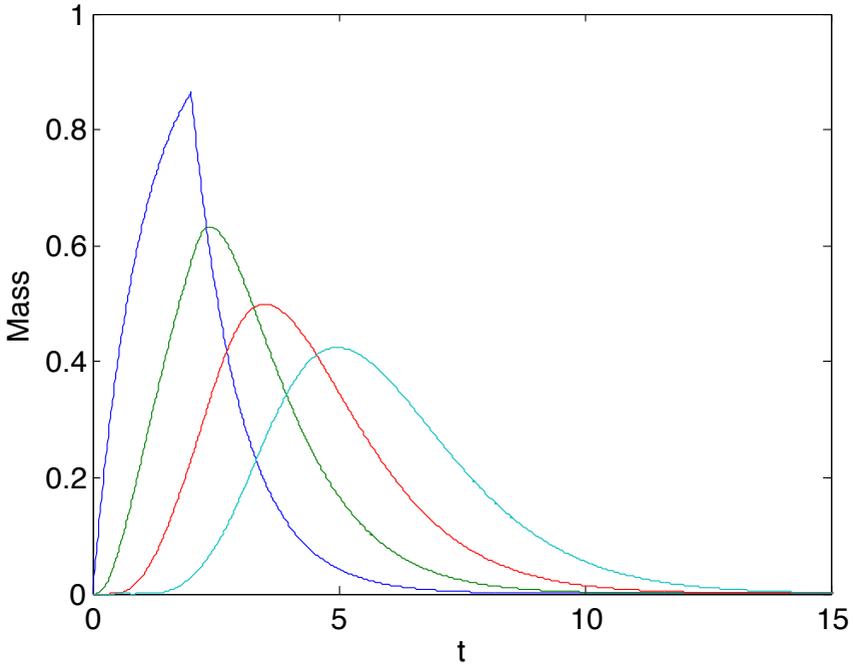
Figure 2:   Solutions of equations (1)–(4) with feed of 1 unit per unit time for $0 \leqslant t \leqslant 2$, all $d_i = 0$, all $a_i = 1$ and $x_i(0) = 0$. Stages one to four are coloured blue, green, red and cyan, respectively.

3   Properties of the solutions

Even with the delay terms included, for constant a_i and initial masses set to zero the solutions behave as if the differential equations are linear. Since they are autonomous, the delay times are removed from each equation by a change of origin, producing constant coefficient linear differential equations. The solutions are linear combinations of exponentials and the sequential nature of the model offers the possibility of the mass transfer rates being determined in turn since a change in the mass transfer rate at stage $i + 1$ leaves the contributions from stages 1 to i unaltered. Moving from one stage to the next
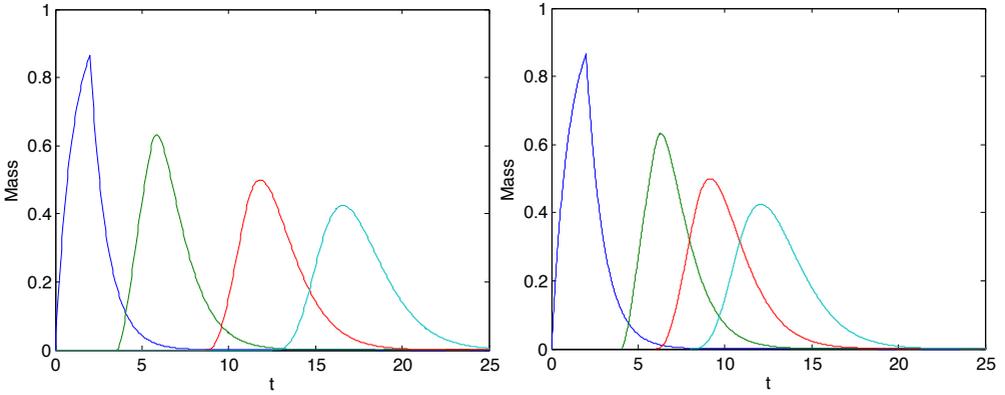
Figure 3: Samples of plots with (left) delays set by volume criteria of 90%, 90% and 50%, and (right) time delays of 4, 6 and 8 time units. Feed is 1 unit per unit time for $0 \leqslant t \leqslant 2$ with all $d_i = 0$ and all $a_i = 1$. Stages one to four are coloured blue, green, red and cyan, respectively.

introduces a further exponential term. It is potentially difficult to determine the rates if a larger rate follows a smaller one. This is because the exponents of the exponentials are all negative and those with the smallest rate will persist longest. This is exemplified by the plots A, B and C in Figure 4. In plot A, the mass transfer rates are all unity, per unit time. In plot B, the mass transfer rate for the third stage is reduced to 0.5, with the remainder unchanged. The solutions for stages one and two are identical but for stage three the retention time (the length of the interval on which the mass is nonzero) is extended, and this persists in stages four and five. In plot C, where only the third mass transfer rate is increased from 1 to 2, the later retention times are largely unaffected. In all three plots the volume activation level is set to 50%. From plots B and C, the magnitudes of the masses moving past a particular location are also affected by the changing mass transfer rates. This property of the solutions is discussed further in Section 4.

Analytical expressions for the solutions of this class of problem and numerical experience from running simulations with up to eight stages suggest that the
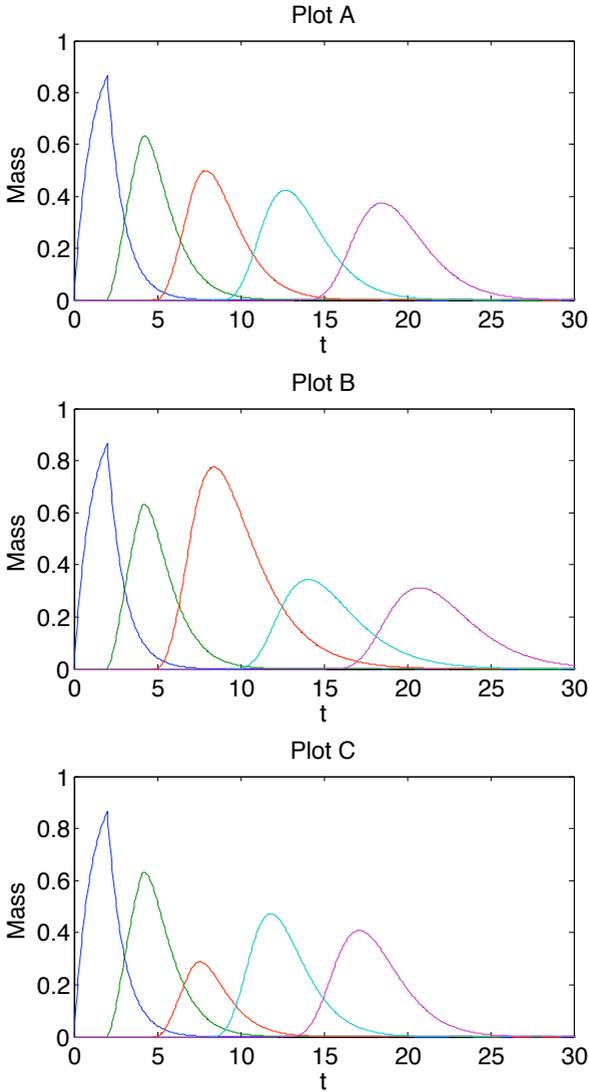
Figure 4: Comparative plots showing the behaviour of a five stage system for differing mass transfer rates with volume criteria of 50%. Feed is 1 unit per unit time for $0 \leqslant t \leqslant 2$. The transfer rates are $a_i = 1$ per unit time for $i = 1, 2, 4, 5$ in all three plots, and $a_3 = 1, 0.5, 2$ per unit time in plots A, B, and C, respectively. Stages one to five are coloured blue, green, red, cyan and magenta, respectively.

Table 1: Two examples of the first seven prescribed mass transfer rates and corresponding calculated retention times in an eight stage system closed with $a_8 = 0$.

Mass transfer rates	1.0	1.00	1.00	0.33	0.10	0.067	0.067
Scaled inverse retention times	1.0	0.80	0.68	0.37	0.15	0.093	0.074
Mass transfer rates	1.0	1.00	1.00	0.19	0.043	0.033	0.067
Scaled inverse retention times	1.0	0.80	0.68	0.25	0.078	0.052	0.047

mass transfer rates a_i of equations (1)–(4) are inversely proportional to the retention times. The latter are somewhat arbitrary since it is necessary to assign a threshold to the mass when estimating a retention time. In practice the advice of the experimentalists is required. In spite of this uncertainty it appears that this relationship provides a good initialisation for a root finding algorithm to estimate mass transfer rates from retention times. Table 1 gives two examples of the inverses of retention times tabulated against the mass transfer rates used to generate the retention times. Since the hypothesis is only a statement about the relative sizes of these quantities, the first entry in the retention times is scaled to unity.

There is no change of mass as the digesta moves through the system, thus the integrated transfer rates should equal the total input. This is verified by direct calculation and is addressed in the next section. An informative approach is to integrate the differential equations (1)–(4) from $t = 0$ to ∞. When the solutions are decaying exponentials

$$x_i(\infty) - x_i(0) = 0 = a_{i-1} \int_0^\infty x_{i-1} \, dt - a_i \int_0^\infty x_i \, dt, \qquad (5)$$

which expresses the equality of the total input and total output masses through the ith node. When $i = 1$ the first term on the right side is the total input f. The contribution of the delay term is included with the first term on the right hand side. Strictly the integration should go from d_{i-1}, but since the value of x_{i-1} is not passed to stage i until $t > d_{i-1}$ equation (5) is valid

for d_i both zero and nonzero. Equation (5) holds when there are no delays and we showed that this analysis remains valid when delays are present.

4   Quantifying the delay terms

Since the markers are inert, the total mass in the system should be conserved when the system is closed; this is the situation when the last mass transfer rate a_n is zero. The four stage plots of Figures 2 and 3 have a_4 nonzero so that all the mass is transported out of the system. In Figure 5, where $a_4 = 0$, the last (cyan) plot is an asymptote of the total mass input since the masses in the other stages fall to zero. It appears that it is only when t gets very large that the sum of the masses equals the input mass, but this is caused by the time delays. By computing the quantities of mass held up by the delays d_i we verify below that mass conservation is assured at all times. As the terms in equations (1)–(4) are mass transfer rates, we obtain the masses by integration. The masses in all stages are zero at $t = 0$ thus integrating the equations and adding them up to stage p, since all masses after stage p are zero at time $T < d_p$,

$$
\begin{aligned}
m_{\text{plots}}(T) &= x_1(T) + x_2(T) + \cdots + x_p(T) \\
&= \int_0^T [f(t) - a_1 x_1(t) + a_1 x_1(t - d_1) - a_2 x_2(t) \\
&\quad + \cdots + a_{p-1} x_{p-1}(t - d_{p-1}) - a_p x_p(t)]\, dt \\
&= \int_0^T f(t)\,dt - a_1 \int_0^{d_1} x_1(t)\,dt - a_2 \int_0^{d_2} x_2(t)\,dt - \cdots - a_p \int_0^T x_p(t)\,dt .
\end{aligned}
\tag{6}
$$

The mass input, $m_{\text{input}}(T)$, say, is the first term on the right side of equation (6) and thus, after some rearranging,

$$
m_{\text{input}}(T) - m_{\text{plots}}(T) = a_1 \int_0^{d_1} x_1\, dt + a_2 \int_0^{d_2} x_2\, dt + \cdots + a_p \int_0^T x_p\, dt .
\tag{7}
$$

Thus the mass which is not accounted for by the plots is the sum of the terms on the right hand side of equation (7),

$$m_{\text{delayed}}(T) = a_1 \int_0^{d_1} x_1 \, dt + a_2 \int_0^{d_2} x_2 \, dt + \cdots + a_p \int_0^T x_p \, dt \,. \qquad (8)$$

and

$$m_{\text{input}}(T) = m_{\text{plots}}(T) + m_{\text{delayed}}(T) \,. \qquad (9)$$

Figure 5 shows the situation for a four stage model with an input of 1 unit per unit time over 2 units of time so that $m_{\text{input}} = 2$. With the use of equation (7), for each value of p the masses held back at each stage are evaluated. The solid line plots in Figure 5 are those of the individual masses and the dashed red plot is the delayed mass m_{delayed}. The times when each stage commences are shown by the black vertical lines, these are the times at which the digesta enters each stage. As a consequence of equation (9), the sum of the solid line plots m_{plots} plus the dashed plot m_{delayed} equals the mass input m_{input}, which is 2 units in Figure 5.

5   Steady state analysis

The previous considerations concerned a single feeding event. As stated earlier, the experimental data concerns a situation in which one marker is fed to a pig on a regular basis. This situation is envisaged as one in which there is a constant input to the system. Intuitively, when the transients die away there will be a constant mass at each stage. We denote the steady state mass by

$$x_i^{\text{ss}} = \lim_{t \to \infty} x_i(t) \,, \qquad (10)$$

and note that

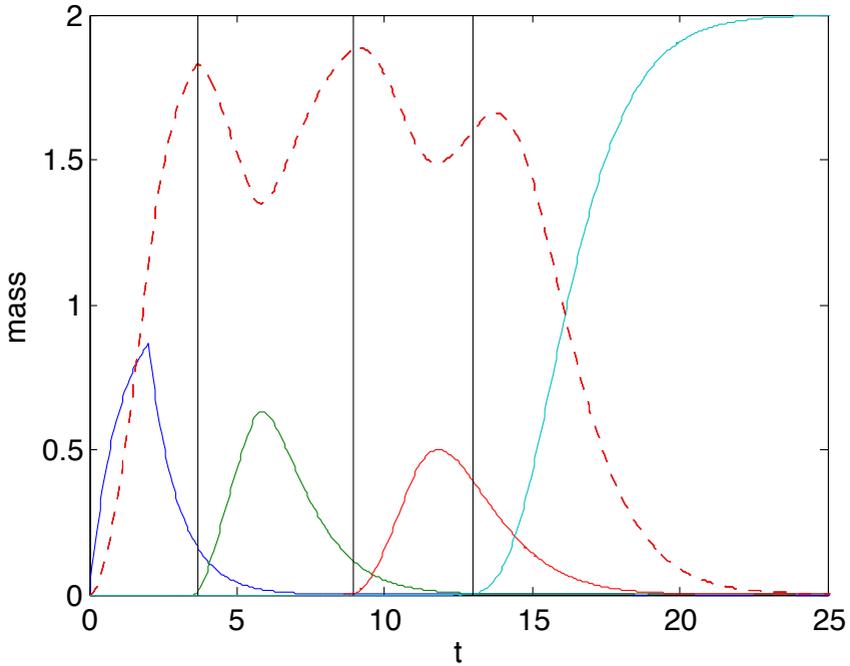$$\lim_{t \to \infty} x_i(t - d_i) = x_i^{\text{ss}} \,, \qquad (11)$$

Figure 5: Plots of the masses for stages one to four (solid lines) and the 'delayed mass' (dashed line) held back by the delay mechanism. Feed is 1 unit per unit time for $0 \leqslant t \leqslant 2$, $a_1 = a_2 = a_3 = 1$ and $a_4 = 0$. Stages one to four are coloured blue, green, red and cyan, respectively. Black vertical lines are at the delay times of 4, 8 and 12 units.

so that, since dx_i/dt goes to zero,

$$0 = a_{i-1}x^{ss}_{i-1} - a_i x^{ss}_i \, , \tag{12}$$

for $i = 2, 3 \ldots$, and, for $i = 1$,

$$0 = \lim_{t \to \infty} f(t) - a_1 x^{ss}_1 \, . \tag{13}$$

Thus we have the values of the steady state masses and how they are related to the rate constants. Even in the time dependent phase, the effect of the
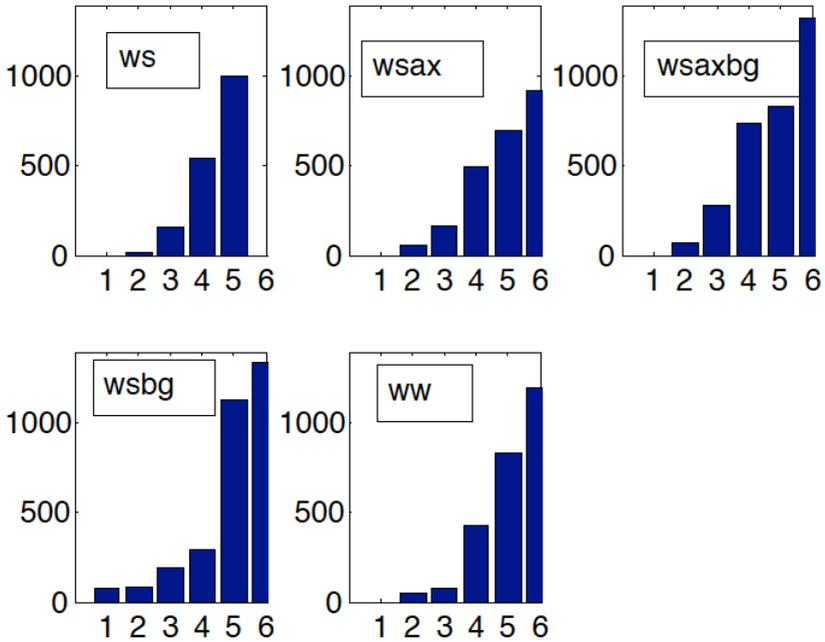
Figure 6: Mass present at the steady state stage of the feeds. Bar plots of the mean mass over each diet in the six stages of the small intestine.

rates on the magnitudes of the masses is observed, for example, on the single input time dependent plots of Figure 4.

Experimental data following the slaughter of the animals was recorded for 30 animals fed five different diets but with an identical marker compound; each small intestine was divided into six parts of similar sizes. The mass at the time of slaughter was recorded for each part (or stage), these are the values of the steady state masses, x_i^{ss}, of equation (10).

The five bar charts in Figure 6 summarise experimental results obtained by averaging the pigs with the same diet. The different diets are WS, WSAX, WSBG, WSAXBG and WW. While the small intestine from each of the pigs was always divided into six stages, biological variation led to some missing values

(i.e., no digesta present in that section of that pig), consequently an average was taken from each diet. We observe some structure, which varies with the diets, and, from the heights of the bar charts, by application of equations (12) and (13), we have information on the ratios of the mass transfer rates.

6   Conclusion

The analysis of a functional–structural model established the properties which the model will capture and what it will predict. Results showed the effects of the rate constants and of delay terms. An important result is the relationship between the steady state behaviours in different compartments from which information on the mass transfer rates can be deduced. These results will be used to analyse data from further markers used for short time information. Very similar methods will also be used for the stomach and small intestine. When this procedure is validated for consistency and reliability, extensions permitting feedback and interactions across processes will be investigated. It is anticipated that the modelling will introduce delay and nonlinear phenomena, as well as other issues [1, 5, 6, e.g.].

References

[1] M. Renton, J. Hanan and K. Burrage, Using the canonical modelling approach to simplify the simulation of function in functional-structural plant models. *New Phytologist*, 166:845–857, 2005. doi:10.1111/j.1469-8137.2005.01330.x C632, C643

[2] D. Bastianelli, D. Sauvant and A. Rerat, Mathematical modeling of digestion and nutrient absorption in pigs. *J. Animal Science*, 74:1873–1887, 1996. http://www.journalofanimalscience.org/content/74/8/1873.abstract C632, C633, C634

[3] R. G. Lentle and P. W. M. Janssen, Manipulating Digestion with Foods designed to Change the Physical Characteristics of digesta. *Critical Reviews in Food Science and Nutrition*, 50:130–145, 2010. doi:10.1080/10408390802248726 C631

[4] J. France, J. H. M. Thornley, M. S. Dhanoa and R. C. Siddons, On the mathematics of digesta flow kinetics. *Journal of Theoretical Biology*, 113:743–758, 1985. doi:10.1016/S0022-5193(85)80191-0 C632

[5] A. Mazanov and J. V. Nolan, Simulation of the dynamics of nitrogen metabolism in sheep. *British Journal of Nutrition*, 35:149–174, 1976. doi:10.1079/BJN19760017 C632, C643

[6] A. Mazanov, Stability of Multi-pool Models with Lags. *Journal of Theoretical Biology*, 59:429–442, 1976. doi:10.1016/0022-5193(76)90181-8 C632, C643

Author addresses

1. **J. A. Belward**, QCSCM and The University of Queensland, Centre for Nutrition and Food Sciences, Queensland 4072, Australia.
   mailto:john.belward@qcscm.com

2. **J. S. Hanan**, The University of Queensland, Centre for Nutrition and Food Sciences, Queensland 4072, Australia.

3. **B. A. Williams**, The University of Queensland, Centre for Nutrition and Food Sciences, Queensland 4072, Australia.

4. **W. J. J. Gerrits**, Animal Nutrition, Wageningen University, Netherlands.

5. **M. J. Gidley**, The University of Queensland, Centre for Nutrition and Food Sciences, ARC Centre of Excellence in Plant Cell Walls, Queensland 4072, Australia.